Application of a habitat-based model to estimate effective longline fishing effort and relative abundance of Pacific bigeye tuna (*Thunnus obesus*)

KEITH A. BIGELOW,[1,*] JOHN HAMPTON[1] AND NAOZUMI MIYABE[2]

[1]*Oceanic Fisheries Programme, Secretariat of the Pacific Community, B.P. D5, 98848 Noumea Cedex, New Caledonia*
[2]*Division of Pelagic Fish Resources, National Research Institute of Far Seas Fisheries, 5-7-1 Orido, Shimizu-shi, Shizuoka-ken, Japan*

ABSTRACT

A new habitat-based model is developed to improve estimates of relative abundance of Pacific bigeye tuna (*Thunnus obesus*). The model provides estimates of 'effective' longline effort and therefore better estimates of catch-per-unit-of-effort (CPUE) by incorporating information on the variation in longline fishing depth and depth of bigeye tuna preferred habitat. The essential elements in the model are: (1) estimation of the depth distribution of the longline gear, using information on gear configuration and ocean currents; (2) estimation of the depth distribution of bigeye tuna, based on habitat preference and oceanographic data; (3) estimation of effective longline effort, using fine-scale Japanese longline fishery data; and (4) aggregation of catch and effective effort over appropriate spatial zones to produce revised time series of CPUE. Model results indicate that effective effort has increased in both the western and central Pacific Ocean (WCPO) and eastern Pacific Ocean (EPO). In the WCPO, effective effort increased by 43% from the late 1960s to the late 1980s due primarily to the increased effectiveness of effort (deeper longline sets) rather than to increased nominal effort. Over the same period, effective effort increased 250% in the EPO due primarily to increased nominal effort. Nominal and standardized CPUE indices in the EPO show similar trends – a decline during the 1960s, a period of stability in the 1970s, high values during 1985–1986 and a decline thereafter. In the WCPO, nominal CPUE is stable over the time-series; however, standardized CPUE has declined by ~50%. If estimates of standardized CPUE accurately reflect relative abundance, then we have documented substantial reductions of bigeye tuna abundance for some regions in the Pacific Ocean. A decline in standardized CPUE in the subtropical gyres concurrent with stability in equatorial areas may represent a contraction in the range of the population resulting from a decline in population abundance. The sensitivity of the results to the habitat (temperature and oxygen) assumptions was tested using Monte Carlo simulations.

Key words: bigeye tuna, circulation models, habitat models, longline fishery, relative abundance

INTRODUCTION

Bigeye tuna (*Thunnus obesus*) is the main target species of the longline fishery in the tropical and subtropical Pacific Ocean, with catches of 90 000–165 000 tonnes since 1980 (Hampton *et al.*, 1999). Stock assessments have been conducted using indices of abundance, nonequilibrium production models, cohort analysis and yield-per-recruit analyses (Miyabe, 1995; Hampton *et al.*, 1998; IATTC, 1999). Central to each method is the use of longline fishery catch and effort statistics to construct indices of bigeye tuna abundance based on CPUE.

Catch of bigeye tuna from longlines is strongly affected by the fishing depth of the gear (Hanamoto, 1987; Boggs, 1992), with gear fishing deeper in the water column being generally more effective in catching bigeye tuna. This catch at depth relationship is thought to be because of a preference of bigeye tuna for temperatures cooler than those of the upper mixed layer (Hanamoto, 1987; Holland *et al.*, 1990; Boggs, 1992; Brill, 1994). Since the mid-1970s, longliners changed their fishing methods from mainly 'conventional' sets (5–6 hooks between mainline floats) fishing a depth range of approximately 90–150 m, to 'deep'

*Correspondence. e-mail: keith.bigelow@noaa.gov
Received 16 October 2000
Revised version accepted 27 July 2001

sets (> 10 hooks between floats) fishing a depth range of approximately 100–250 m (Suzuki *et al.*, 1977; Hanamoto, 1987). This switch increased the effectiveness of longline gear in catching bigeye tuna, with possibly greater efficiency gains in the western and central Pacific Ocean (WCPO), where the optimum temperature range of bigeye tuna is considerably deeper than in the eastern Pacific Ocean (EPO). Conversely, the concentration of dissolved oxygen (DO) that limits bigeye tuna vertical distribution (Brill, 1994) may be sufficiently shallow in some areas to impact the effectiveness of longline fishing.

The variation in fishing depths of longlines and the depth of the preferred habitat can be used to standardize longline CPUE in order to provide an unbiased estimator of bigeye tuna relative abundance. Hinton and Nakano (1996) presented a method of estimating 'effective' longline effort using the distribution of 'nominal' effort' and information based on habitat preferences and constraints, in combination with environmental data. In this paper, we have developed a new application of the habitat-based model to estimate effective longline effort and standardize CPUE for Pacific bigeye tuna caught by Japanese longliners in the Pacific Ocean. In some regions of the Pacific, significant declines in relative abundance as indicated by standardized CPUE were not apparent in the corresponding nominal CPUE time series because of changes in the effectiveness of fishing effort. Monte Carlo simulations were used to estimate the variability of the results due to uncertainty in assumptions regarding bigeye tuna habitat preferences.

METHODS

Effective fishing effort

We define effective fishing effort (f) in a particular area (indexed by a) and time (indexed by t) stratum as the weighted sum of longline hooks (E) fishing in different depth zones (indexed by d) throughout the vertical habitat:

$$f_{at} = E_{at} \sum_{d} h_{atd}\, p_{atd} \tag{1}$$

where h_{atd} is the proportion of hooks fishing in depth zone d in area a during time period t and p_{atd} is the proportion of bigeye tuna in area a during time period t occurring in depth zone d. In this analysis, we used 15 depth bins of 40 m (range, 0–600 m) to define the vertical habitat. The data analysed were those from the Japanese longline fleet operating in the Pacific Ocean for the period 1966–96 stratified by 1°-square areas and by quarter. Although longline vessels from other nations (e.g. Taiwan, Korea and the United States) have also operated in the Pacific Ocean for several decades, we chose to use the Japanese fleet and associated data for this analysis because (1) it has consistently targeted tuna over a large area of the Pacific Ocean; (2) the data resolution is generally better than that of other fleets; (3) catch and effort by this fleet represents the largest component of the longline fishery in the Pacific Ocean; and (4) ancillary information on approximate fishing depth is also available from the Japanese fleet.

The key elements in the estimation of effective longline effort are the specification of the depth distribution of the gear (h_{atd}) and the depth distribution of bigeye tuna (p_{atd}). These aspects of the analysis are discussed in the following two sections.

Depth distribution of longline gear

Predicting hook depth distribution from gear configuration

The actual depth at which longline gear fishes is known to be influenced by the set configuration, such as the number of hooks between floats, floatline and branchline lengths, distance between branchlines, sagging rate of the mainline (Fig. 1) and a variety of environmental factors, particularly wind and currents (Suzuki *et al.*, 1977; Boggs, 1992; Mizuno *et al.*, 1998, 1999). The depth of the longline is typically altered by varying the length of mainline between floats and the sagging rate of the mainline [ratio of horizontal distance between two floats and the stretched length of mainline between two floats (Suzuki *et al.*, 1977)]. While actual fishing depth has been measured in several studies with time-depth-recorders (TDRs)

Figure 1. Configuration of a pelagic longline. h_a is length of branch line, h_b is length of float line, HL is the horizontal length between two floats, L is half of the length of the mainline between two floats and ϕ is the angle between the horizontal and tangential line of the mainline.

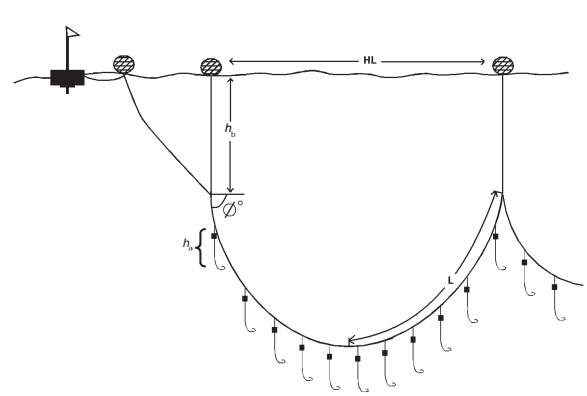

(Boggs, 1992; Uozumi and Okamoto, 1997; Mizuno *et al.*, 1998, 1999), fishing depth measurements are rarely available from commercial longline sets. However, the number of hooks between adjacent mainline floats (HBF), which is routinely recorded on Japanese longline logbooks, can be used along with other information on set configuration to estimate the approximate depth distribution of longline hooks using catenary geometry (Suzuki *et al.*, 1977):

$$D_j = h_a + h_b + L\left\{(1+\cot^2\phi)^{1/2} - \left[\left(1-2\frac{j}{N}\right)^2 + \cot^2\phi\right]^{1/2}\right\} \quad (2)$$

where D_j is the depth of the j-th hook, h_a is the length of the branch line, h_b is the length of the float line, L is half of the length of the mainline between two floats, N is HBF + 1, j is the j-th branch line from the float line, and ϕ is the angle between the horizontal and tangential line of the mainline. The parameter is solved by iteration of the sagging rate (HL/2 L, Fig. 1).

The catenary parameters $\{h_a = 26.3$ m, $h_b = 19.4$ m, $L = [(50\text{ m})*(\text{HBF} + 1)/2]$, $\phi = 60°$, sagging rate $= 0.72\}$ were estimated from data collected by at-sea observers deployed on Japanese vessels (212 longline sets) in the 1990s (unpublished observer data, SPC, BP D5 98848, Noumea Cedex, New Caledonia). Thus, using equation 2 it is possible to estimate the depth of longline hooks for various HBF categories.

From 1966 to 1996, gear configuration in the Japanese longline fishery ranged from 3 to 22 HBF. Yellowfin or bigeye tuna longline sets were usually conducted by day fishing at moderate (100–250 m) to deep depths (100–400 m) with gear of five HBF or greater. Data corresponding to 3–4 HBF were deleted prior to analysis because these shallow gear types were used mainly to target swordfish at night. For the purpose of determining approximate hook depth distributions, the remaining HBF information were aggregated into six categories: 5–6 HBF (regular gear), 7–9 HBF (intermediate gear), and 10–11, 12–15, 16–20 and 21–22 HBF (deep gear).

Between-set and within-set variability

The catenary estimation results in a single depth estimate for each longline hook; however, actual hook depths vary both between and within longline sets. We characterized between-set hook-depth variability for each HBF value by randomly generating 1000 values of ϕ from a normal distribution ($\mu = 60°$, $\sigma = 11.3°$, unpublished data, SPC) and computing D_j for each.

Within-set variability in longline fishing depth has been estimated using TDR data (Boggs, 1992; Yano and Abe, 1998). Boggs (1992) observed that the deepest hook on a longline set has the greatest movement and calculated a 30% variation (~100 m) in settled depth of the deepest hook on a set deployed to > 300 m. Similarly, Yano and Abe (1998) found a linear increase in depth fluctuation as hooks were deployed deeper. Based on data from Yano and Abe (1998), the relationship between the standard deviation of hook depth D_j and hook number j (the hooks closest to the floats are numbered 1) was:

$$\sigma(D_j) = 8.73 + 4.4j \quad (r^2 = 0.64) \quad (3)$$

Within-set variability in D_j was characterized by generating 500 random samples of hook depths from normal distributions of mean D_j and standard deviation $\sigma(D_j)$ for each of the 1000 estimates of D_j obtained previously; thereby producing 500 000 estimates of D_j for each HBF value of five through 22. Aggregate hook-depth distributions (40-m depth bins) corresponding to the six HBF categories were produced by aggregating the individual hook distributions within those categories (Fig. 2).

Effect of currents

Boggs (1992) observed that hook depths were usually shallower (54–68%) than those predicted from catenary geometry, especially in deep sets (> 300 m). Reasons for shallow set depths include wind and currents, with current shear between the surface and thermocline being of paramount importance. Although it is certain that wind and currents shoal longline gear, there is little published quantitative information available on this effect. We have used available published and unpublished data (Uozumi and Okamoto, 1997; Bach[1], Mizuno *et al.*, 1998, 1999) to estimate longline shoaling as a function of surface current velocities of 0–60 cm s^{-1}:

$$S = 0.985V \quad (r^2 = 0.28) \quad (4)$$

where S is the shoaling percentage and V is the absolute (u and v vectors combined) current velocity in m s^{-1}.

[1]Bach, P. (1997) Etude du comportement de la palangre pour la mise en œuvre de tactiques de filage. Texte de l'exposé présenté à l'occasion de Rencontres de la Pêche Hauturière, Papeete, Les 5 et 6 mai 1997.

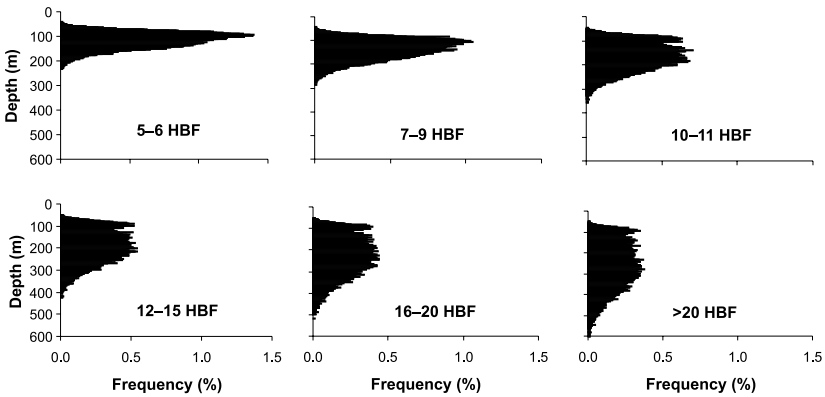

Figure 2. Distribution of hook depth in six gear configurations within the Japanese tuna longline fishery. HBF = hooks between floats.

A time-series (1980–96) of oceanic currents was obtained from an Ocean Global Circulation Model (OGCM) developed at the National Center for Environmental Prediction (NCEP, Behringer *et al.*, 1998). The model has 27 vertical layers (0–3000 m) and a spatio-temporal resolution of 1.5° by one month. Data for each layer were aggregated by quarter and re-gridded to 1° to correspond with the fishery data. The initial eight layers (0–80 m) of the model were averaged to provide current velocity in the mixed layer above the thermocline. Prior to 1980, the OGCM was used to make an average quarterly climatological series. The generic distributions of hook depths for each HBF category shown in Fig. 2 were adjusted for each area-time stratum in the model by the following equation:

$$\mathbf{D}' = \mathbf{D} - \mathbf{D}\left[\frac{S}{1 + \exp[a(\mathbf{D} - D_{0.5})]}\right] \quad (5)$$

where $\mathbf{D}'$ is the depth distribution after adjustment for current velocity, a is a parameter defining the slope of the function, $\mathbf{D}$ is the depth distribution prior to adjustment, and $D_{0.5}$ is the median depth at the inflexion point of hook depth distribution. Equation 5 was empirically determined from four longline sets (13 HBF) that monitored effects of currents on individual hook depths between successive floats (Uozumi and Okamoto, 1997; Mizuno *et al.*, 1999). A value of −0.025 was chosen for the curvature parameter a to provide realistic shoaling results over the range of hook depths. Values less than −0.025 had less shoaling of shallower hooks and greater shoaling of deeper hooks (cf. −0.025, −0.05 and −0.075, Figure 3). The inflexion point of the relationship was at $D_{0.5}$. Theoretical estimates of hook depth based on equations 4 and 5 were accurate to approximately 20 m when compared to observed data. The application of the methodology described above produced estimates of h_{atd} that incorporated the combined effects of longline set configuration, between-set and within-set variability in hook depth distribution, and the shoaling effects of ocean currents on hook depth distribution. The shoaling of longline gear was most evident from 10°S to 15°N in the area of equatorial currents and countercurrents.

Figure 3. Illustration of the various curvatures based on parameter a in equation 5 for shoaling of longline gear 11–12 hooks between floats with a current velocity of 0.4 m sec^{-1}. A value of –0.025 (solid line) was used in the model.

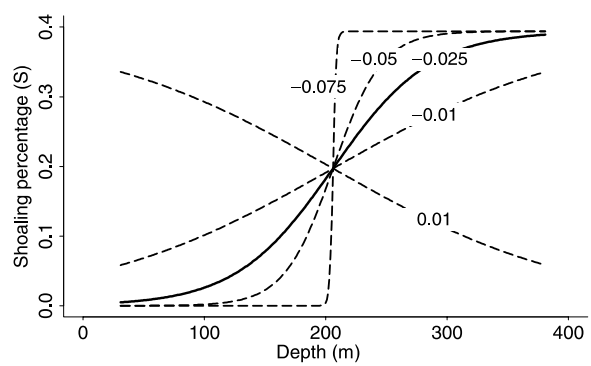

Bigeye tuna habitat preferences as determinants of depth distribution

Unlike other species of tuna and billfish (Block *et al.*, 1992; Brill *et al.*, 1993; Brill *et al.*, 1999), the depth distribution of bigeye tuna appears to be directly related to ambient temperature preference (rather than a sea surface-ambient temperature differential) and minimum dissolved oxygen (ml l^{-1}) requirements. In our application of a habitat-based model bigeye depth distribution is based on ambient temperature, rather than previous applications of the model that limited blue marlin (Hinton and Nakano, 1996) and swordfish (Hinton and Deriso, 1998) populations at temperatures relative to the mixed layer. Temperature preferences of bigeye tuna were inferred from the

results of archival (electronic data recording) tag and acoustic tracking studies on fish > 30 kg (Dagorn *et al.*, 2000; Musyl *et al.*, in press) which are equivalent to the size of longline-caught bigeye tuna.

Both daytime and nighttime temperature distributions (Fig. 4) were used to formulate temperature preference hypotheses. Japanese tuna longline gear is typically deployed in the early morning, allowed to soak for 8–10 h and retrieved throughout the afternoon and evening. Observer data (219 longline sets) indicate that about 75% of soak time occurs during the day and 25% at night. Therefore, the bigeye tuna temperature preference distributions for day and night were combined using 0.75 and 0.25 as weighting factors for day and night, respectively, to obtain an initial overall temperature preference distribution (expressed on a scale of 0–1, Fig. 5a).

Physiological experiments, longline monitoring and tracking studies provide information about bigeye tuna DO preferences. Physiological observations indicate that bigeye tuna cardiac performance is reduced at DO concentrations < 2.1 ml l^{-1} (Bushnell *et al.*, 1990), consistent with longline monitoring studies that suggested that adult bigeye are rarely caught in water with DO ranging from 1.0 to 1.4 ml l^{-1} (Hanamoto, 1987; Boggs, 1992). In the tropical and subtropical western and central Pacific, DO concentrations are high over most of the temperature range preferred by bigeye tuna; therefore, DO is unlikely to limit vertical distribution in this region. In contrast, DO concentration in the EPO is much lower at a given depth than in the WCPO. As an initial preference hypothesis, a DO index (again on a scale of 0–1) was constructed in which bigeye tuna were not limited at DO > 2.25 ml l^{-1}. This index declines linearly from 2.5 to 0.5 ml l^{-1} and is zero at < 0.5 ml l^{-1} (Fig. 5b).

Figure 4. Time-at-temperature histograms for adult bigeye tuna during day (a) and night (b). Data are from Hawaii (Musyl *et al.*, in press) and Tahiti (Dagorn *et al.*, 2000).

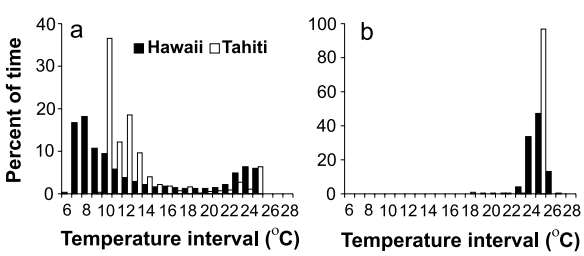

Figure 5. Distribution (scale of 0 to 1) of temperature (a) and oxygen (b) assumptions for Monte Carlo simulation. Solid line indicates the initial temperature and oxygen hypotheses and the shaded area indicates the range of the hypotheses used in the simulation.

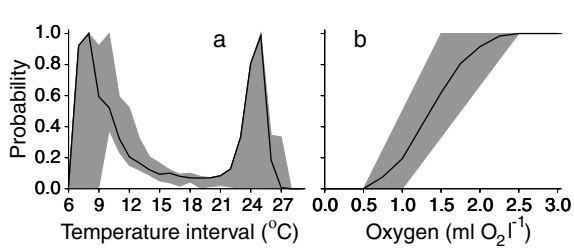

Bigeye tuna habitat quality was defined as the product of the scaled temperature and DO indices. Values of this combined index, normalized to sum to one across the 15 40-m depth bins, were used to specify p_{atd}, the relative vertical distribution of bigeye tuna at each area-time stratum (1° by quarter). A time-series of temperature data obtained from the OGCM (with pre-1980 represented by a quarterly climatology) was used to generate the temperature indices. Model verification and ground truthing was evident from the good correspondence between independent temperature-at-depth measurements (mooring records) and OGCM output for the 20°C isotherm at three locations (165°E, 140°W, 110°W) along the equator (Ji and Smith, 1995).

Dissolved oxygen profile data were obtained from a climatological database (Levitus and Boyer, 1994). These data summarize the spatial and seasonal variability of DO at depth averaged over a long period of time (1934–94). Ultimately, it would be preferable to use time-specific data to account for interannual variability in DO, but such data are not currently available at the spatial and temporal coverage required for this analysis.

Computing aggregate effective effort and relative abundance

The estimates of h_{atd} and p_{atd} allow for the estimation of effective effort from nominal effort using equation 1. Standardized CPUE, or relative abundance, may then be determined at 1° quarter resolution simply by C_{at}/f_{at} , where C_{at} is the catch (in number of bigeye tuna) in a 1° square *a* during quarter *t*.

For stock assessment purposes, it may be useful to aggregate f_{at} and C_{at} into larger area and time strata according to the requirements of the assessment. We aggregated effective effort and standardized CPUE observations into years according to two spatial aggregation schemes: (1) the WCPO and EPO separated at 150°W longitude (an informal boundary currently used for tuna stock assessment in the Pacific) and (2) eight bio-ecological provinces (Fig. 6), based on primary productivity regimes (Longhurst *et al.*, 1995). Standardized CPUE values occurring in a particular

Figure 6. Bio-ecological provinces used to spatially aggregate longline effort and relative abundance indices (after Longhurst *et al.*, 1995). NPST – west – North Pacific Subtropical Gyre (west), NPST – east – North Pacific Subtropical Gyre (east), NPTG – North Pacific Tropical Gyre, WARM – Western Pacific Warm Pool, PNEC – North Pacific Equatorial Countercurrent, PEQD – Pacific Equatorial Divergence, ARCH – Western Pacific Archipelagic Deep Basins, SPSG – South Pacific Subtropical Gyre. In addition to the bio-ecological provinces, the western and central Pacific Ocean (WCPO) and eastern Pacific Ocean (EPO) are separated at 150°W.

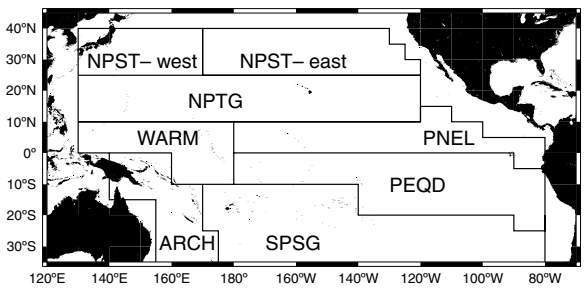

year and geographical region can be weighted by area (geographical size of a 1° square) or fishing effort (Hinton and Nakano, 1996). We present results based on the median values of area-weighted squares, although similar results were obtained using an effort-weighted scheme. Implicit in either case is the assumption that the observations randomly 'sample' relative abundance within that year by region.

Sensitivity analysis

Monte Carlo simulations were used to assess the impact of uncertainty in our habitat assumptions on the estimates of effective effort and relative abundance. Ten alternative hypotheses were generated for both temperature and oxygen preferences based on our interpretation of their uncertainty (Fig. 5, Table 1). Estimation of effective effort and relative abundance was repeated 1000 times, in each case randomly selecting from the 10 temperature-preference and 10 DO-preference hypotheses with equal likelihood. Uncertainty in relative abundance was represented by plotting the 2.5, 50 and 97.5 percentiles of the Monte Carlo iterations. The long-term mean of standardized CPUE was normalized to a value 1.0 to facilitate comparison with nominal CPUE estimates.

RESULTS AND DISCUSSION

Modelled population distribution

Vertical profiles on two meridional sections (at 160°E and 120°W) of temperature habitat quality, DO habitat quality, combined temperature–DO habitat quality and p_{atd} are depicted in Fig. 7 for our initial temperature and oxygen hypotheses. The distribution of habitat preferences agrees well with a previous fisheries oceanography study (Hanamoto, 1987).

Table 1. Bigeye tuna temperature hypotheses used in Monte Carlo simulations. Hypotheses are based on archival tag data from Hawaii (Musyl *et al.*, in press) and acoustic tracking in Tahiti (Dagorn *et al.* 2000).

Hypothesis	Assumption
1 – Hawaii	100% day + 25% night
2 – Hawaii	100% day + 10% night
3 – Hawaii	100% day + 40% night
4 – Hawaii	100% day
5 – Hawaii	100% day + 2°C
6 – Hawaii	100% day with no feeding at warm temperatures
7 – Tahiti	100% day + 10% night
8 – Tahiti	100% day + 25% night
9 – Tahiti	100% day + 40% night
10 – Tahiti	100% day

In the western Pacific at mid-latitudes (160°E section) temperature habitat values are low (<0.4) at depths shallower than 400 m. Near the equator, an index value of 0.4 occurs at shallower depths (~250 m) indicating that the model would distribute the population shallower at the equator than at mid-latitudes. Temperature habitat values are shallower in the EPO (120°W section) compared to the WCPO as a value of 0.4 typically occurs at <300 m at most latitudes. From 20°S–20°N in the WCPO (160°E) and 5–10°N in the EPO (120°W), there is an absence of bigeye in the upper 100 m because the temperature is too warm. In both meridional sections, the high index values at shallow depths (<200 m) indicate the mix of daytime (deeper, colder) and nighttime (shallower, warmer) distributions used in the analysis.

Along 160°E at 5–15°N, DO is limiting at depths > 200 m. Along 120°W, DO is limiting at depths as shallow as 100 m in tropical waters north of the equator. The combination of temperature and DO preferences indicates that the bigeye would be mostly distributed by the model at depths greater than 300 m in the WCPO, except around the equator where it is 200-300 m. In the EPO, bigeye are distributed in the upper 200 m from 10°S to 20°N due to DO limitation at depth. The bigeye habitat is progressively deeper at higher latitudes in both the north (200–300 m) and south Pacific (>400 m).

Figure 7. Meridional (160°E and 120°W) and zonal (10°N) sections of bigeye tuna habitat indices for temperature, oxygen, combined temperature and oxygen and normalized habitat quality (p_{jky}). Habitat indices follow initial temperature and oxygen hypotheses in Fig. 5.

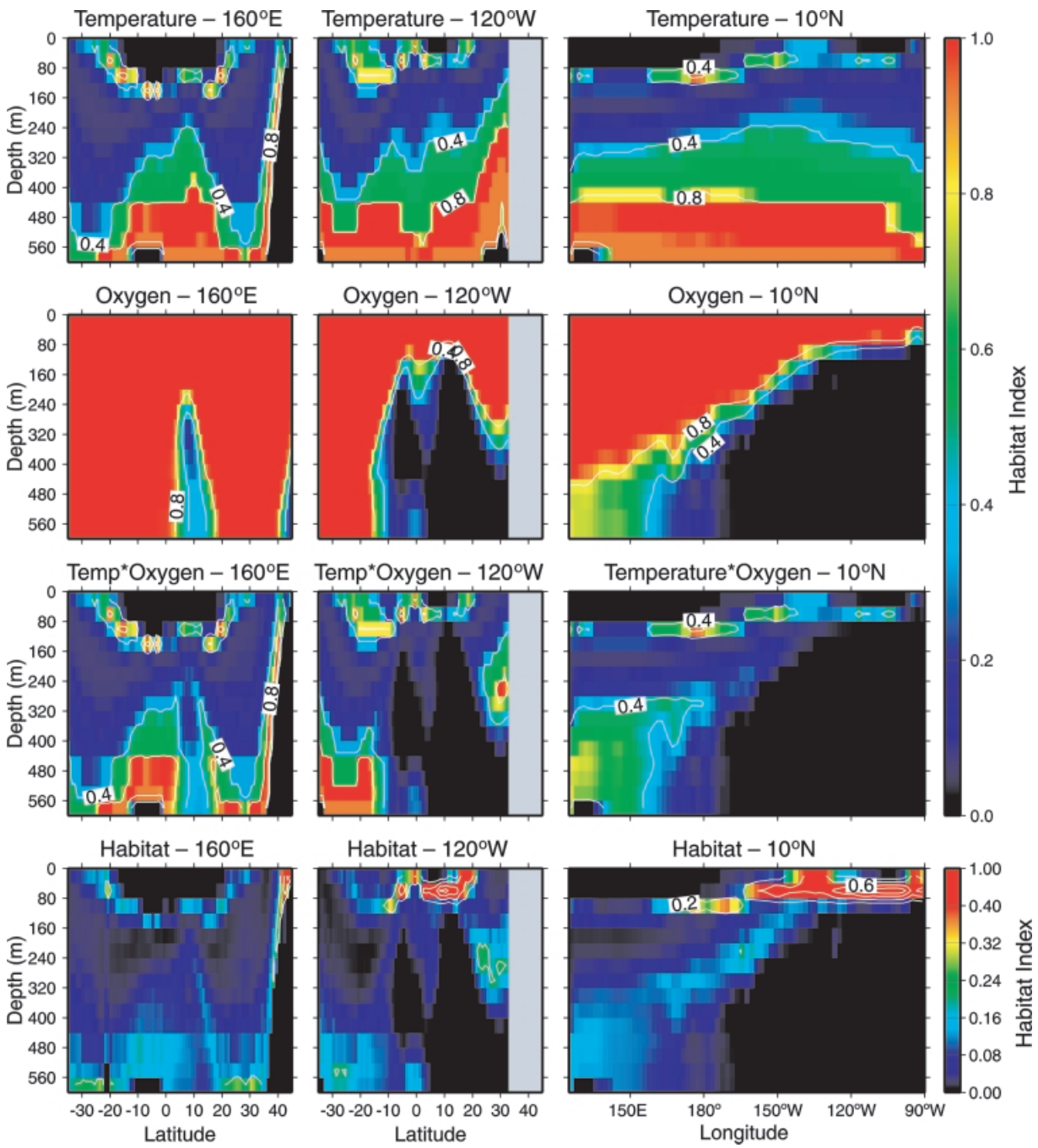

Moving east, bigeye habitat is progressively confined to the upper layers because of shallower DO-deficient water.

The percentage of the bigeye population in the upper 300 m, as inferred from the p_{atd} estimates, is illustrated for the entire Pacific Ocean in Fig. 8. In the WCPO, the population distribution is shallow at lower latitudes ~10°N, gradually deepens at mid-latitudes and shoals again at high (~40°) latitudes. In the EPO, the predicted population distribution occurs in

Figure 8. Percentage of bigeye population from 0 to 300 m inferred from the habitat-based model. Bigeye are distributed according to initial temperature and oxygen hypotheses in Fig. 5. The western and central Pacific Ocean (WCPO) and eastern Pacific Ocean (EPO) are separated at 150°W for comparison.

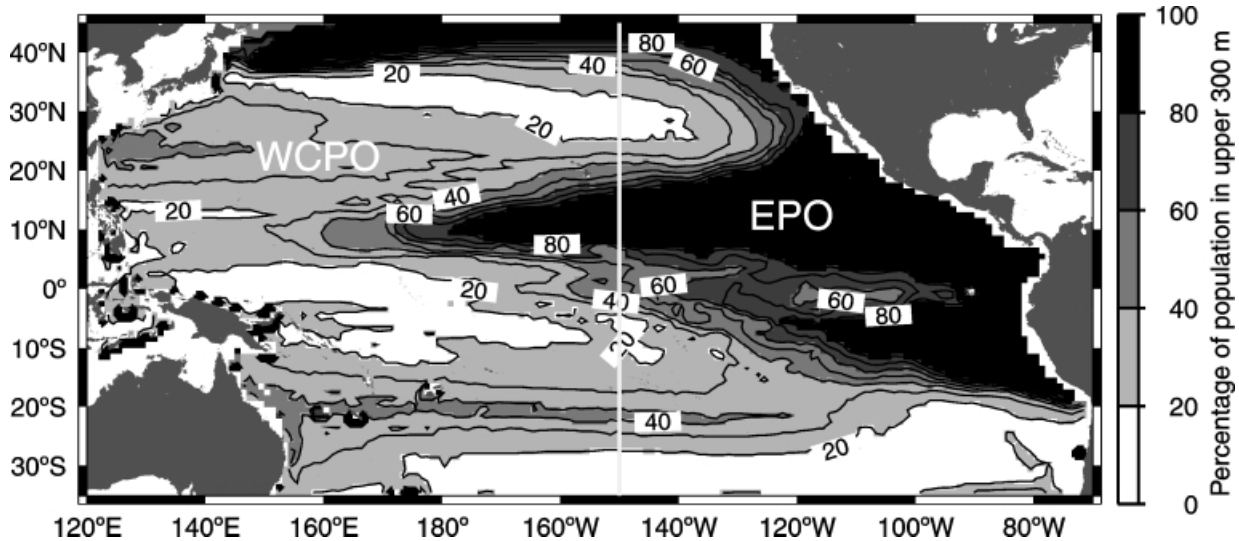

shallower water than in the WCPO. Bigeye are distributed deeper at higher latitudes in the EPO, such as in the North Pacific Transition Zone. There is also a reduction of bigeye in the upper 300 m at subtropical and temperate latitudes in the south Pacific.

Effective effort

Trends in effective effort have increased in both the WCPO and EPO (Fig. 9). In the WCPO, effective effort increased 43% from the late 1960s to the late 1980s. Over the same period, effective effort increased 250% in the EPO. Effective effort has declined in the EPO since the early 1990s because of vessels leaving the fishery. Effective effort as a percentage of nominal effort increased ~50% in the WCPO over the time-series (Fig. 9). In contrast, effective effort as a percentage of nominal effort in the EPO has remained stable. Nominal effort in the WCPO has declined since the 1960s; however, effective effort actually increased because of greater targeting of the bigeye habitat. There was a steady increase in nominal effort within the EPO until the early 1990s.

Throughout the time-series there was an increase in effective effort in four of the eight bio-ecological

Figure 9. Annual effective longline effort (shaded area is 95% confidence intervals) and effective effort as a percentage of total nominal effort (line with circles) in the bigeye tuna habitat for the western and central Pacific Ocean (WCPO) and eastern Pacific Ocean (EPO).

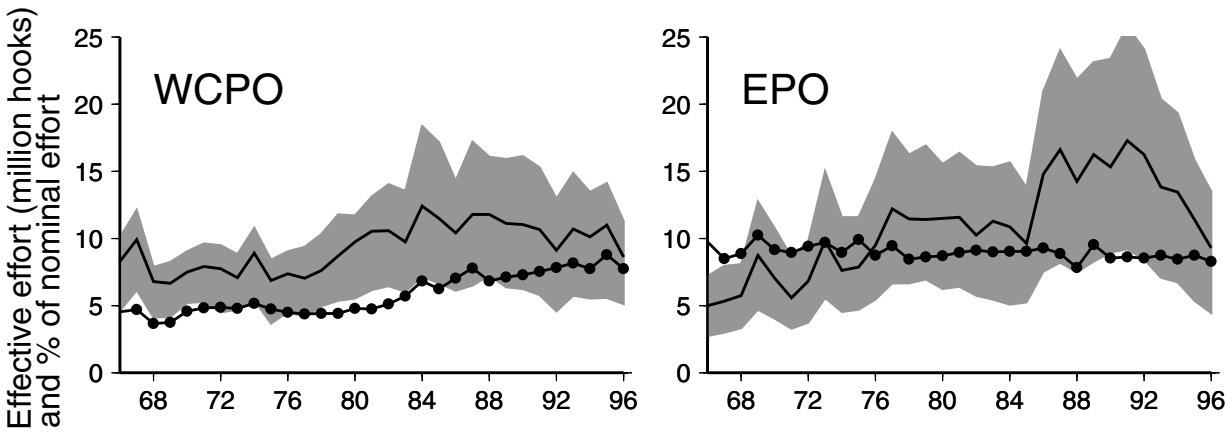

provinces with the remaining four provinces remaining stable (Fig. 10). Annual estimates of effective effort were highest for the equatorial provinces (PNEL and PEQD), moderate for the warm pool, tropical and subtropical gyres in the north Pacific [western Pacific warm pool (WARM), north Pacific tropical gyre (NPTG) and NPST-east] and lowest in the western subtropical gyres in the western north Pacific and subtropical south Pacific [NPST-west, western Pacific archipelagic basin (ARCH), south Pacific subtropical gyre (SPSG)]. The greatest effective effort is expended in the Pacific Equatorial Divergence (PEQD), a traditional fishing ground for the Japanese longline fleet. Effective effort in this province increased five-fold between the late 1960s and early 1990s. Gear modifications in four provinces (NPST-west, NPST-east, NPTG and WARM) indicated that the longline was more efficient in the bigeye habitat after 1980.

Relative abundance

The north Pacific shows the greatest temporal changes with a substantial standardized CPUE reduction in the subtropical (18°–32°N) area during the 1980s and 1990s (Fig. 11). The subtropical south Pacific does not show a similar decline, but this interpretation is complicated because the Japanese fleet has not actively fished this area due to limited fishing access arrangements and presumably because of the thermal profile, whereby bigeye are more difficult to catch.

Trends in standardized CPUE differed from nominal CPUE for the WCPO, but were similar for the EPO (Fig. 12). The 95% confidence intervals of

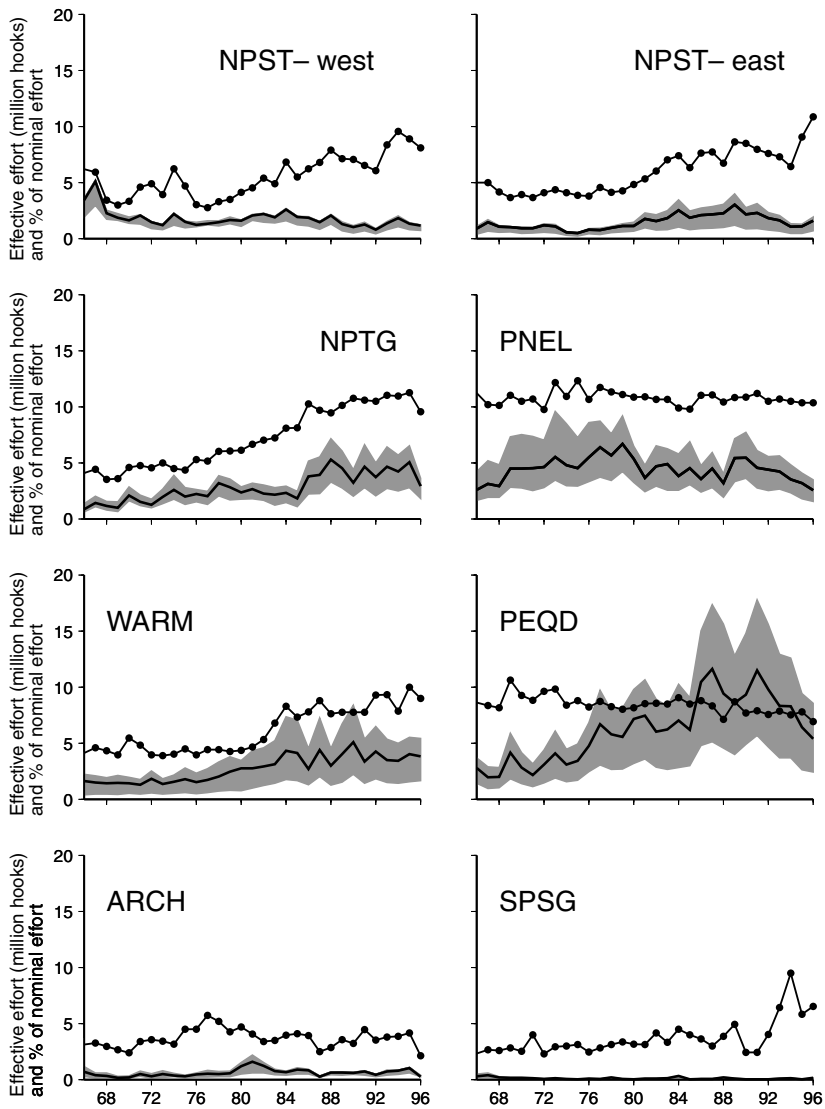

Figure 10. Annual effective longline effort (shaded area is 95% confidence intervals) and effective effort as a percentage of total nominal effort (line with circles) in the bigeye tuna habitat in the eight bio-ecological provinces in the Pacific Ocean. Figure 6 illustrates the bio-ecological provinces.

Figure 11. Spatial comparison of bigeye standardized CPUE in the Japanese longline fishery during the last four decades.

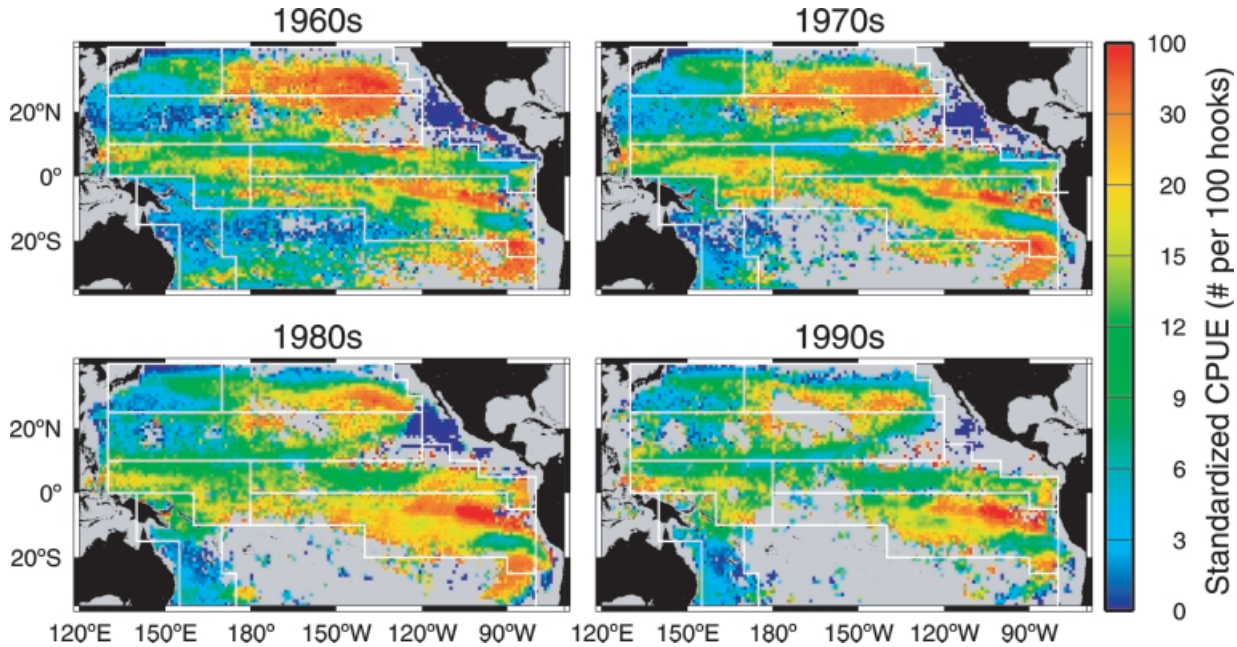

standardized CPUE were wider for the WCPO and median annual standardized CPUE from simulations declined continuously since 1978 (Fig. 12). The wider confidence intervals in the WCPO may result from the greater abundance of islands, which may create microhabitat effects on standardized CPUE. The divergence between nominal and standardized CPUE in the WCPO results from progressive changes in longline fishing characteristics (shift to deeper sets) of the Japanese fleet, which resulted in longline effort becoming more efficient in the WCPO because of better targeting of optimal bigeye habitat. For the EPO, both nominal and standardized indices show similar trends – a decline during the 1960s, a period of stability in the 1970s, high values during 1985 and 1986 and a decline thereafter. The similarity between indices results from the shallower habitat for bigeye in the EPO and a less dramatic change to deeper sets as in the WCPO. Thus, the model has less of a standardization effect in the EPO, because there has been a smaller relative impact on longline effort efficiency.

Figure 12. Annual nominal CPUE (line with circles) and standardized CPUE (relative abundance) estimates for bigeye tuna in the western and central Pacific Ocean (WCPO) and eastern Pacific Ocean (EPO). Monte Carlo simulations account for the variation in habitat preference assumptions and illustrate the median standardized CPUE for each year and 95% confidence intervals (shaded area). Time-series of standardized CPUE is normalized to a value of 1.0.

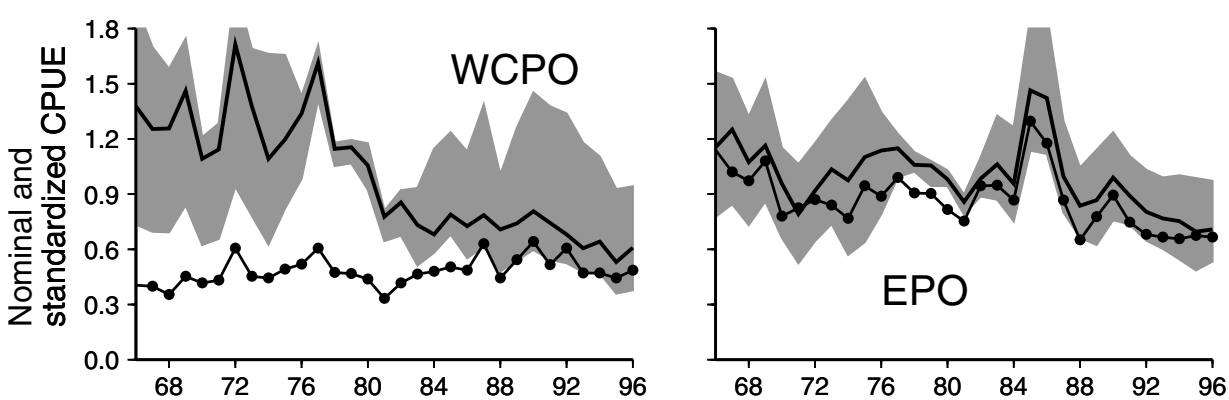

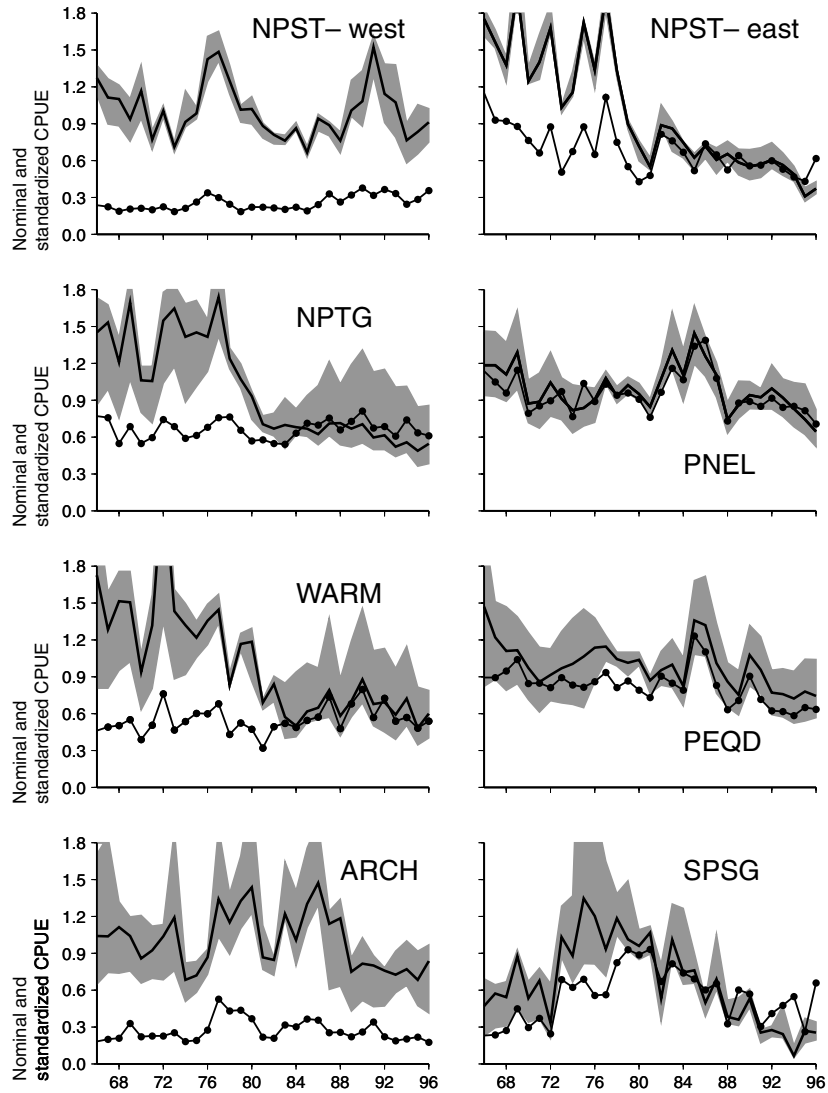

Figure 13. Annual nominal CPUE (line with circles) and standardized CPUE (relative abundance) estimates for bigeye tuna in eight bio-ecological provinces in the Pacific Ocean. Figure 6 illustrates the bio-ecological provinces. Monte Carlo simulations account for the variation in habitat preference assumptions and illustrate the median standardized CPUE for each year and 95% confidence intervals (shaded area). Time-series of standardized CPUE is normalized to a value of 1.0.

Stratification by the bio-ecological provinces may be preferable to a simple east–west stratification as it may better characterize large-scale spatial variation in bigeye tuna abundance. Of the eight provinces, nominal CPUE was stable in six and declined in two (Fig. 13). In comparison, standardized CPUE declined in four and was stable in four. Within the subtropical gyres of each hemisphere (NPST-east and SPSG), the decline in standardized CPUE from the 1970s to the 1990s was more precipitous (~70%) than nominal CPUE (~50%). There was no apparent decline in standardized CPUE in the subtropical gyre in the NPST-west or the ARCH; however, these regions have the lowest catch rates of the eight provinces. Nominal CPUE was stable in the NPTG and WARM; however, standardized CPUE declined at a rate similar to the subtropical gyres (~70%). The two provinces in the equatorial central and western Pacific (PNEL and PEQD) had high nominal and standardized CPUE in the 1980s, though values in the 1990s were below average levels for the entire time-series.

CONCLUSIONS

The application of habitat-based models to the estimation of effective fishing effort and relative abundance involves several assumptions. The most critical of these is that the tagging (archival and acoustic) and physiological data adequately characterize adult bigeye habitat. Monte Carlo simulation quantified the model outputs given the effects of uncertainty in habitat assumptions, although the inputs were based on small sample sizes. By using a variety of habitat assumptions, one can assess how these uncertainties progress

through the model and affect trends in relative abundance. Within the model, habitat assumptions and associated oceanographic data specify bigeye tuna vertical distribution. This underscores the value of physiological, behavioural, and environmental data in interpreting longline fishery catch and effort. We framed our bigeye tuna temperature preference hypotheses on the basis of archival or acoustic tracking studies from two geographical areas in the Pacific, but additional data are needed to adequately characterize behavioural variability related to the environment, fish size and other factors.

Assumptions regarding the depth distribution of longline gear considered combined effects of set configuration, between-set and within set variability in hook distribution and shoaling effects due to ocean currents. The prediction of hook depth from gear configuration was fairly realistic; however, adjusted hook depths due to gear shoaling by surface (0–80 m) current velocities may be biased because the relationship was poorly correlated ($r^2 = 0.28$). The shoaling of longline gear may be affected by other factors such as wind and current shear between the surface layer and thermocline, but inclusion of these factors was beyond the scope of the study. While uncertainty exists in the relationship, the shoaling effect does not emerge as a particularly sensitive parameter in the model as it was only evident in areas of high current velocity (10°S–15°N) and assumptions of bigeye habitat were more important for standardizing longline effort.

The habitat-based model could be applied to additional fisheries that exploit bigeye tuna with appropriate modifications to the habitat assumptions. The current application of model is based on a longline fishery operating mainly during the daytime. The model could be applied to other fleets that conduct night longline fishing, such as the Hawaii-based longline fleet and the mainland Chinese fleet operating in Micronesia. The probability distributions on the habitat assumptions would therefore be altered to reflect the nighttime behavior of bigeye. The spatio-temporal resolution of the present model was 1° square and quarter, but the model could be extended to incorporate lunar effects and associated cloud cover for fisheries with finer temporal scale data. The habitat assumptions would be altered to reflect that bigeye have behavioral differences within the lunar cycle as the nighttime distribution of fish is deeper during full moon than new moon (Musyl *et al.*, in press).

If our estimates of standardized CPUE accurately reflect relative abundance, then we have documented substantial reductions of bigeye tuna abundance for some regions in the Pacific. Despite a concentration of effective longline effort in the PEQD, both nominal and standardized CPUE declined by only 25%, suggesting that fishing performance has been maintained while fishing effort dramatically increased. In contrast, standardized CPUE has declined severely in other areas (WARM, NPTG and NPST-east), with modest increases in effective effort. The standardized CPUE reduction in the subtropics concurrent with stability in equatorial areas may represent a contraction in the range of the population resulting from a decline in abundance.

Several species groups (e.g. fish, birds, insects, and mammals) have shown differential habitat utilization given changes in abundance. MacCall (1990) reviewed the concept of 'density-dependent habitat selection', in which population size is an important factor that influences the choice of ecological habitat or the relative distribution of the population. Population expansion or contraction can depend on effective population size. Population contractions usually occur at the frontiers of the population, which for bigeye tuna would be high latitude areas such as the subtropical gyres. Similar to skipjack and yellowfin tunas, the centre of the bigeye tuna population may be located in equatorial waters where local density can be maintained (PNEL and PEQD) despite contractions or expansions in peripheral habitats.

In conclusion, the use of effective, rather than nominal effort for longline fisheries should provide better information on changes in abundance. In the present model, effective effort accounted for changes in fishing depth adjusted by current velocity, and variability in bigeye tuna preferred habitat, as reflected by temperature and dissolved oxygen concentrations. The model accounted for habitat variability on seasonal, interannual (e.g. El Niño Southern Oscillation) and possibly longer time scales. The model suggests that a large portion of adult bigeye are not amenable to capture in some areas of the Pacific (tropical and subtropical gyres) because they are distributed deeper than the depth at which most longline gear can be set.

ACKNOWLEDGEMENTS

We gratefully acknowledge our colleagues who provided the data used in this study. In particular, the Japan National Research Institute of Far Seas Fisheries for fisheries data, C. Boggs (National Marine Fisheries Service) and M. Musyl (Joint Institute of Marine and Atmospheric Research) for the Hawaii archival tag data, L. Dagorn (Institut de Recherche pour le Développment, Montpellier, France) for acoustic tracking data and M. Ji (National Center for Envi-

ronmental Prediction) for Ocean Global Circulation Model outputs. Funding assistance was provided by the Australia Agency for International Development. We also thank M. Hinton, M. Musyl and anonymous reviewers for their comments on the manuscript.

REFERENCES

Behringer, D.W., Ji, M. and Leetmaa, A. (1998) An improved coupled model for ENSO prediction and implications for ocean initialization. Part I: The ocean data assimilation system. *Mon. Wea. Rev.* **126**:1013–1021.

Block, B.A., Booth, D.T. and Carey, F.G. (1992) Depth and temperature of the blue marlin, *Makaira nigricans*, observed by acoustic telemetry. *Mar. Biol.* **114**:175–183.

Boggs, C.H. (1992) Depth, capture time, and hooked longevity of longline-caught pelagic fish: timing bites of fish with chips. *Fish. Bull. U.S.* **90**:642–658.

Brill, R.W. (1994) A review of temperature and oxygen tolerance studies of tunas pertinent to fisheries oceanography, movement models and stock assessments. *Fish. Oceanogr.* **3**:204–216.

Brill, R.W., Block, B.A., Boggs, C.H., Bigelow, K.A., Freund, E.V. and Marcinek, D.J. (1999) Horizontal movements and depth distribution of large adult yellowfin tuna (*Thunnus albacares*) near the Hawaiian Islands, recorded using ultrasonic telemetry: implications for the physiological ecology of pelagic fishes. *Mar. Biol.* **133**:395–408.

Brill, R.W., Holts, D.B., Chang, R.K.C., Sullivan, S., Dewar, H. and Carey, F.G. (1993) Vertical and horizontal movements of striped marlin (*Tetrapturus audax*) near the Hawaiian Islands, determined by ultrasonic telemetry, with simultaneous measurement of oceanic currents. *Mar. Biol.* **117**:567–574.

Bushnell, P.G., Brill, R.W. and Bourke, R.E. (1990) Cardiorespiratory responses of skipjack tuna (*Katsuwonus pelamis*), yellowfin tuna (*Thunnus albacares*), and bigeye tuna (*Thunnus obesus*) to acute reductions of ambient oxygen. *Can. J. Zool.* **68**:1857–1865.

Dagorn, L., Bach, P. and Josse, E. (2000) Movement patterns of large bigeye tuna (*Thunnus obesus*) in the open ocean determined using ultrasonic telemetry. *Mar. Biol.* **136**: 361–371.

Hampton, J., Bigelow, K. and Labelle, M. (1998) A summary of current information on the biology, fisheries and stock assessment of bigeye tuna (*Thunnus obesus*) in the Pacific Ocean, with recommendations for data requirements and future research. Sec. Pacific Comm., Oceanic Fish. Prog. Technical Report. No. 36, pp. 46.

Hampton, J., Lewis, A. and Williams, P. (1999) The western and central Pacific tuna fishery: 1998 overview and status of stocks. Sec. Pacific Comm., Oceanic Fish. Prog., Tuna Fish. Ass. Report. No. 1, pp. 39.

Hanamoto, E. (1987) Effect of oceanographic environment on bigeye tuna distribution. *Bull. Jpn. Soc. Fish. Oceanogr.* **51**:203–216.

Hinton, M.G. and Deriso, R.D. (1998) Distribution and stock assessment of swordfish, *Xiphias gladius*, in the eastern Pacific Ocean from catch and effort data standardized on biological and environmental parameters. In: *Biology and Fisheries of Swordfish, Xiphias gladius* (Papers from the International Symposium on Pacific Swordfish, Ensenada, Mexico, 11–14 December 1994), I. Barrett, O. Sosa-Nishizaki, and N. Bartoo (eds). NOAA Technical Report NMFS **142:**161–179.

Hinton, M.G. and Nakano, H. (1996) Standardizing catch and effort statistics using physiological, ecological, or behavioral constraints and environmental data, with an application to blue marlin (*Makaira nigricans*) catch and effort data from Japanese longline fisheries in the Pacific. *Inter-Am. Trop. Tuna Comm. Bull.* **21**:171–200.

Holland, K.N., Brill, R.W. and Chang, R.K.C. (1990) Horizontal and vertical movements of yellowfin and bigeye tuna associated with fish aggregating devices. *Fish. Bull. U.S.* **88**:493–507.

IATTC (1999) *Assessment of bigeye tuna in the eastern Pacific Ocean*. Background Paper 5, 63rd Meeting of the IATTC, La Jolla, 8–10 June.

Ji, M. and Smith, T.M. (1995) Ocean model response to temperature data assimilation and varying surface wind stress: intercomparison and implications for climate forecast. *Mon. Wea. Rev.* **123**:1811–1821.

Levitus, S. and Boyer, T. (1994) *World Ocean Atlas. 1994*, Vol. *2: Oxygen. NOAA Atlas NESDIS 2*. Washington, D.C.: U.S. Government Printing Office.

Longhurst, A., Sathyendranath, S., Platt, T. and Caverhill, C. (1995) An estimate of global primary production in the ocean from satellite radiometer data. *J. Plankton. Res.* **17**:1245–1271.

MacCall, A.D. (1990) *Dynamic Geography of Marine Fish Populations*. Seattle and London: University of Washington Press.

Miyabe, N. (1995) Follow-up study on the stock status of bigeye tuna in the Pacific Ocean. *Working Paper 12, 5th Meeting of the Western Pacific Yellowfin Research Group, Noumea,* 21–23 August, New Caledonia, pp. 15.

Mizuno, K., Okazaki, M. and Miyabe, N. (1998) Fluctuation of longline shortening rate and its effect on the underwater longline shape. *Bull. Far Seas Fish. Res. Lab.* **35**:155–164.

Mizuno, K., Okazaki, M., Nakano, H. and Okamura, H. (1999) Estimating the underwater shape of tuna longlines with micro-bathythermographs. *Inter-Am. Trop. Tuna Comm., Special Report* **10**, pp. 35.

Musyl, M.K., Brill, R.W., Boggs, C.H., Curran, D.S., Kazama, T.K. and Seki, M.P. (in press). Vertical movements of bigeye tuna (*Thunnus obesus*) associated with islands, buoys, and seamounts of the Hawaiian Archipelago from archival tagging data.

Suzuki, Z., Warashina, Y. and Kishida, M. (1977) The comparison of catches by regular and deep tuna longline gears in the western and central equatorial Pacific. *Bull. Far Seas Fish. Res. Lab.* **15**:51–89.

Uozumi, Y. and Okamoto, H. (1997) Research on the hook depth of longline gear in the 1995 research cruise of the R/V Shoyo Maru. *Working Paper 3, 7th Meeting of the Western Pacific Yellowfin Research Group,* 18–20 June, Nadi, Fiji, pp. 20.

Yano, K. and Abe, O. (1998) Depth measurements of tuna longline by using time-depth recorder. *Nippon Suisan Gakkaishi* (in Japanese, with English abstract) **64**:178–188.